

## Molecular-dynamics study of surface relaxation, stress, and disordering of Pb(110)

C. P. Toh and C. K. Ong

*Department of Physics, National University of Singapore, Kent Ridge, Singapore 0511*

F. Ercolessi

*International School for Advanced Studies, Via Beirut 4, I-34014 Trieste, Italy*

(Received 11 July 1994)

Using an empirical many-body Hamiltonian fitted to bulk and surface properties of lead, we have studied the temperature-dependent structural transformations on Pb(110) by molecular-dynamics simulation. The surface is observed to undergo an anomalous thermal expansion prior to disordering at  $T \sim 500$  K, in good agreement with recent ion-scattering and low-energy electron-diffraction studies. Behavior of the layer-resolved structure factors indicates that the disordering process is anisotropic and occurs in a layer-by-layer fashion. Simulation results are also consistent with experimental observations of surface roughening near 400 K as well as the formation of a quasiliquid surface phase above 500 K. The intrinsic stress anisotropy  $\Delta g$ , present on all fcc (110) surfaces, vanishes at  $T \sim 590$  K, suggesting the possible existence of a liquid film at the surface. By examination of the structural-anisotropy data taken at various temperatures, we confirmed that complete melting of the surface layer is achieved at  $\sim 590$  K.

### I. INTRODUCTION

The amount of experimental data on the thermal behavior of the low index lead surfaces has risen steadily for the past few years due to the availability of high-quality Pb single crystals with a minimum amount of subgrain boundaries and other defects. Moreover, lead is a very interesting material in the sense that among all its neighbors in the fourth column of the Periodic Table, it is the only real fcc metal. Moreover, it is extremely ductile, has a low melting temperature and very low vapor pressure, not to mention that it has long acquired an important status in the petrol chemical industries. The fact that it can display a rich variety of surface phenomena as found in recent studies on Pb(110) justifies its popularity as a laboratory test case in the field of surface science.

One of the earliest measurements of surface properties of lead were made on Pb crystallites where it was shown that the surface energy of the (100) face is only slightly larger than that of the (111) face, with the ratio of the two being about 1.02 between 473–573 K.<sup>1</sup> However, the real excitement only began when techniques were devised that facilitated characterization of the surface structure at elevated temperatures. Using low-energy electron diffraction (LEED), Breuer *et al.*<sup>2</sup> investigated the multilayer relaxation of Pb(110) at 130 and 300 K and showed that the first few layer spacing actually exhibited an oscillatory behavior in addition to a strongly compressed surface layer. Strong contraction of the first interlayer spacing was also reported by Li *et al.*<sup>3</sup> from results of LEED analyses. Despite its usefulness, LEED- $I(E)$  measurements which were needed for the spatial determination are practically impossible for  $T > 300$  K due to significant Debye-Waller scattering for Pb(110) above room temperature. Nevertheless, evidence for anomalous thermal expansion at the Pb(110) surface were presented by Frenken, Huussen, and van der Veen<sup>4</sup> using a combination of

ion shadowing and blocking techniques. By employing the same method, Frenken and co-workers<sup>5</sup> showed that surface premelting occurred at about 100 K below the bulk melting point on the same surface (i.e.,  $T_m = 600.7$  K). This observation was supported by x-ray photoelectron diffraction studies<sup>6</sup> where it was found that the angle-dependent forward-scattering enhancements decreased with increasing temperature, at first slowly up to about 500 K, followed by a steep decrease towards  $T_m$ . This steep decrease is interpreted as being due to a massive disordering of the Pb(110) surface, in agreement with the Rutherford backscattering data. The extension of the above investigation to the behavior of the quasiliquid layer (QLL) (Ref. 7) revealed an increasing melt thickness with temperature, which followed first a logarithmic growth law  $|\ln(T_m - T)|$ , then asymptotically a power law  $(T_m - T)^{-r}$ , with  $r = 0.315 \pm 0.015$ . Subsequent studies of the two-dimensional self-diffusion processes at the disordered surface using the quasielastic scattering of low-energy He atoms gave strong indication of directional anisotropy.<sup>8</sup> The results also inferred that at  $T \geq 450$  K, the surface atoms are anomalously mobile and at  $T \geq 550$  K, surface mobilities are found to exceed the bulk liquid value. The high mobility of adatoms was clearly demonstrated by temperature-dependent scanning tunneling microscopy measurements on Pb(110) (Ref. 9) where workers systematically observed a jump to contact with the tip followed by the subsequent buildup of a sizable neck above room temperature.

Another kind of disordering that can occur on loose-packed crystal surfaces is called roughening.<sup>10</sup> Here the atoms still occupy the crystalline positions, while in the premelted surface, crystalline order decays from the crystal-liquid to the liquid-vapor interface. Thermodynamically, the roughening transition is characterized by the vanishing of the step free energy for steps on the facet that roughens up while the conditions for premelt-

ing of a crystal face is given by  $\gamma_{SV} > \gamma_{SL} + \gamma_{LV}$  where the free energies are those for solid-vapor (SV), solid-liquid (SL), and liquid-vapor (LV) interfaces, respectively. Particle growth experiments indicated a roughening of the Pb(110) surface near 390 K.<sup>11</sup> Roughening was also observed by high-resolution low-energy electron diffraction (HRLEED) near 415 K (Ref. 12) where a high density of surface steps is generated. The transition is defined to be of the Kosterlitz-Thouless kind (infinite order) (Ref. 13) in which the surface height-height correlation function diverges logarithmically. It has also been shown that modification of surface structures and roughening phase transition in Pb(110) can result by the addition of impurities.<sup>14</sup> All these suggest that roughening and premelting can occur on the same surface. Current evidence indicates that the pure Pb(110) surface undergoes a roughening transition at  $\sim 400$  K, followed by substantial disordering of the near surface region at  $\sim 525$  K.

Although it is widely accepted that Pb(110) is non-reconstructed, recent findings using different surface probes seem to suggest that this surface is capable of a large variety of ground-state structures ranging from  $(1 \times 1)$ ,  $c(2 \times 4)$ ,  $(1 \times n)$ , and  $(2 \times n)$  to microfaceted, depending upon thermal history.<sup>15</sup> As a further surprise, HRLEED studies by Yang *et al.*<sup>16</sup> have indicated the presence of a novel phase on the Pb(110) surface below 400 K. They believed that the observed surface phase which contains two layers of atoms separated by double steps may be related to a class of disordered flat phases predicted recently by Rommelse and den Nijs.<sup>17</sup> Despite the wealth of information that is available for the Pb(110) surface as seen from the examples above, little has been done on the theoretical side via simulation due to the lack of a realistic model potential. To our knowledge, there is only one molecular-dynamics study on the disordering of Pb(110) using the embedded atom method<sup>18</sup> although it has been also applied with some success to an investigation of the energetics of the formation and migration of defects in Pb(110).<sup>19</sup> However, the potential used in these studies is questionable at high temperatures where anharmonic effects become important as it does not seem to produce the correct melting temperature. In particular, a simulation run at 650 K for 100 psec failed to show complete bulk melting. The objective of this paper is to use a recently proposed "glue" Hamiltonian to study surface relaxation and stress, in addition to elucidating the microscopic mechanism of surface disordering on Pb(110) by molecular-dynamics simulation. In Sec. II, we give a brief description of the glue Hamiltonian and the simulation method. Section III is devoted to a detailed discussion and analysis of the results. This is followed by conclusions in Sec. IV.

## II. METHOD

The two slabs used in this work are made up of 16 (110) layers of  $14 \times 5$  atoms each. One is longer in the [001] direction while the other has a larger dimension in the  $[1\bar{1}0]$  direction. The reason for choosing such an asymmetric cell is that the same samples will be used in a future study on the mechanism of diffusion in a molten

surface along the two orthogonal directions, thus requiring a good resolution in the wave vector to be able to identify the possible local minimum in the full width at half maximum of the dynamic structure factor. Having two small asymmetric samples instead of one large symmetric slab leads to a considerable saving of CPU time, especially in the calculation of the dynamic structure factor. We verified that both samples gave consistent behavior in the high-temperature regime and hence, only one is used in subsequent discussions. Periodic boundary conditions are imposed in the lateral directions to mimic an infinite surface. Atoms belonging to the bottom four layers are held fixed to simulate the infinite bulk. During the heating procedure, the lattice constant of the sample is set to correspond to the simulated temperature according to an independently simulated zero-pressure thermal expansion curve for bulk lead. Atoms in the slab interact through a force field derived from a classical many-body "glue" potential. This method has been applied previously to studies of the structural, dynamical, and thermodynamical behavior of Pb clusters,<sup>20</sup> of the stability of stepped Pb(111) surfaces,<sup>21</sup> and of the interaction between a tip and a surface.<sup>22</sup> A similar potential fitted to gold has also been successfully applied to the study of surface reconstruction and premelting on low index Au surfaces.<sup>23</sup> Briefly, the total potential energy  $V$  for a given arrangement of atoms is given by

$$V = \frac{1}{2} \sum_{\substack{j=1 \\ j \neq i}}^N \phi(r_{ij}) + \sum_{i=1}^N U(n_i), \quad (1)$$

where  $\phi(r)$  is a two-body short-ranged potential and  $U(n)$  is a many-body function that describes the gluing effects of the conduction electrons. The "generalized coordination"  $n_i$  of atom  $i$  is a superposition of some fictitious "atomic charge densities"  $\rho(r_{ij})$ ,

$$n_i = \sum_{\substack{j=1 \\ j \neq i}}^N \rho(r_{ij}), \quad (2)$$

where  $\rho(r)$  is a short-ranged monotonically decreasing function of distance.

The values of the three functions,  $\phi$ ,  $\rho$ ,  $U$ , and their derivatives at some fixed points are determined from fits to experimental quantities while the shapes of these functions far away from the fitting points are "fine tuned" to give a good overall description of the real material by using simulation in the fitting procedure to monitor thermal properties, and by looking at different geometries. This results in a potential with a degree of transferability to different physical situations which is difficult to achieve by traditional fitting schemes. In our case, the potential has been fitted to the cohesive energy, surface energy, elastic constants, phonon frequencies, thermal expansion, and melting temperature, following Ref. 24 for Au. In an independent study, we have determined the thermodynamical melting point to be  $\sim 618 \pm 3$  K which is in reasonable agreement with the experimental value. While details regarding the fit and the melting temperature will be published elsewhere,<sup>25</sup> it is important to note that the surface energy, absolutely crucial for an accurate

description of surface energetics, is one of the fitted quantities (in particular,  $\gamma = 38 \text{ meV}/\text{\AA}^2$  at  $T=0$  for “an average crystal plane” from Ref. 26). Parametrizations based on other fitting schemes often suffer from surface energies much lower than the experimental ones.<sup>27</sup> Despite the emphasis on surface properties, it is encouraging to note that there is good agreement between simulated and experimental values for bulk properties that are not used in the fitting process. For example, the bulk vacancy formation energy calculated with our model potential ( $\sim 0.434 \text{ eV}$ ) is reasonably close to the experimental value of  $0.5 \text{ eV}$ .

The heating procedure is done as follows: We first anneal the newly created samples at  $300 \text{ K}$  using standard molecular dynamics, then execute a quench whereby kinetic energy is continuously extracted from the system until  $T$  becomes very close to zero and forces are negligible. This results in a sample where all layers are optimally relaxed. Following this, the sample is heated to  $100 \text{ K}$  by rescaling the particle velocities at each time step (1 time step =  $7.33 \times 10^{-15} \text{ sec}$ ) for 10 000 steps to adjust the kinetic energy to conform to the desired temperature. A constant energy run is then performed until the temperature, density, and order parameters stabilize. This equilibration period normally last for about 10 000 time steps although it can take up to 20 000 time steps in the high-temperature regime. Finally, we collect statistics averaged over another 5000 time steps from a constant energy run. This procedure is then repeated for various temperatures in the range of  $100\text{--}605 \text{ K}$ . Results presented in the following sections are thus averages over two independent simulation runs, using both samples.

### III. RESULTS AND DISCUSSIONS

#### A. Surface relaxation

The surface relaxation at various temperatures has been determined experimentally by Frenken, Huussen, and van der Veen<sup>4</sup> using ion shadowing and blocking techniques. From the results obtained, they concluded that the thermal expansion coefficient of a Pb crystal is substantially enhanced at its (110) surface, which is evidenced by a decrease in surface contraction with temperature. This can be summarized as follows: At  $29 \text{ K}$ , the net shift  $\Delta d_{1b}/d = \sum_{i=1}^4 \Delta d_{i,i+1}/d$  of the first layer with respect to its truncated bulk position equals  $-(15.4 \pm 2.5)\%$  of the bulk interplanar spacing  $d$ . Upon heating, the contraction decreases (i.e., the surface expands) nonlinearly to  $\Delta d_{1b}/d = -(3 \pm 5)\%$  at  $485 \text{ K}$ , at which temperature the surface becomes partially disordered. The anomalous thermal expansion at a crystal surface was also predicted by Jayanthi, Tosatti, and Pietronero in a theoretical study of Cu surfaces.<sup>28</sup>

To investigate the correlation between the loss of surface contraction and the onset of disordering (premelting), we calculate  $\Delta d_{1b}/d$  at temperatures ranging from  $100$  to about  $450 \text{ K}$ . Our results (see Fig. 1) are in excellent agreement with those obtained by Frenken *et al.*, suggesting that the surface expansion coefficient is not constant, but increases nonlinearly at high temperature.

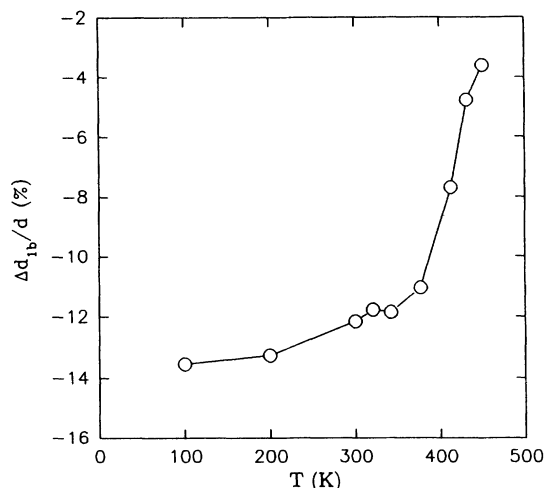


FIG. 1. The temperature-dependent relaxation  $\Delta d_{1b}/d$  of the first layer with respect to its bulk-truncated position.

Unfortunately, efforts to gather more data points at temperatures higher than  $450 \text{ K}$  failed as it becomes increasingly difficult to determine accurately the distance between the first two layers due to frequent exchanges of atoms between them. Analysis of  $z$ -resolved density profiles seems to indicate a vanishing of the surface contraction at  $\sim 500 \text{ K}$ , which incidentally happens to be the point where a quasiliquid layer starts to form in our sample. However, it has been observed recently in simulation<sup>23</sup> and experiment<sup>29</sup> that surface premelting can also occur on Au(110), which possesses a strong ( $\sim 18\%$ ) vertical contraction. Therefore, the anomalous surface expansion of Pb may not be a crucial feature to explain its melting behavior. It is also interesting to note that simulated Au(110) melts without the creation of vacancy-atom pairs that we observe on Pb(110), as shown in the next section.

#### B. Surface disordering

The fourfold orientational order parameter  $O_4$  for the first six layers as a function of temperature is shown in Fig. 2. The definition of  $O_4$  is

$$O_4 = \frac{\left| \sum_{ij} W_{ij} e^{4i\theta_{ij}} \right|}{\sum_{ij} W_{ij}}, \quad (3)$$

where the sums run over first- and second-neighbor pairs and  $\theta_{ij}$  is the angle that the  $i$ - $j$  bond, projected on the  $x$ - $y$  plane, forms with the  $x$  axis. The weight function  $W_{ij}$  is given by

$$W_{ij} = \exp \left[ -\frac{(z_i - z_j)^2}{2\delta^2} \right] \quad (4)$$

with  $\delta$  being half of the average interlayer spacing and has the purpose of filtering out all “noncoplanar” neighbors.  $O_4$  has a value of 1 for a well-ordered surface and

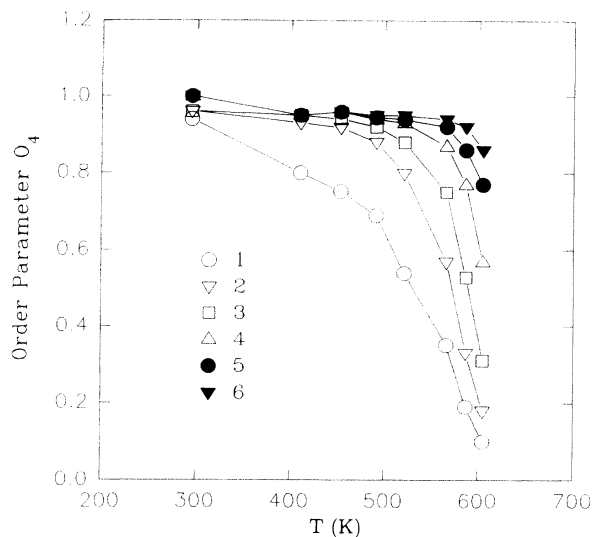


FIG. 2. Orientational order parameter  $O_4$  versus temperature for the first six layers of our sample.

close to 0 for a surface without orientational or short-ranged order like in the case of a bulk liquid. At temperatures below 300 K, a plot of the atomic positions shows that no defects are present. Vacancy-atom pair formation only occurs at 350 K and above, followed by the clustering of adatoms at  $\sim 400$  K (see Fig. 3). Despite the presence of these defects, no anomalous behavior is observed for  $O_4$  in the first layer since atoms still occupy genuine crystalline positions, thus retaining the orientational order of the surface. However, a sharp decrease above 500 K is a clear indication of the onset of premelting whereby the atom arrangement becomes disordered as shown in Fig. 4. This is substantiated by a large cal-

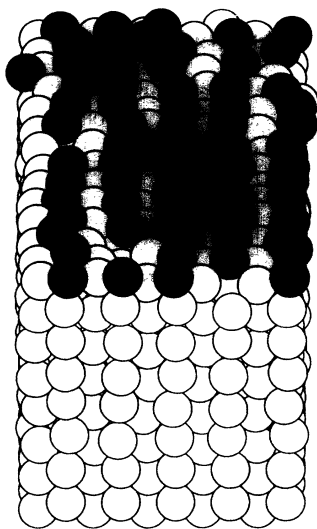


FIG. 3. Snapshot showing the formation of an adcluster along a  $[1\bar{1}0]$  trough at  $T=410$  K. Dark colored balls refer to atoms in the topmost layer.

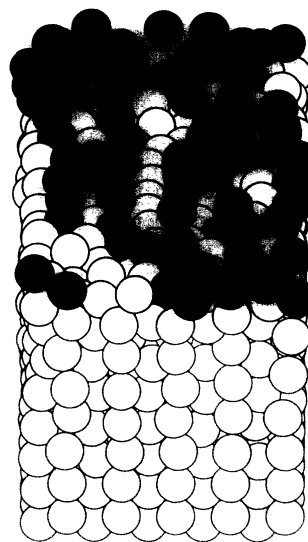


FIG. 4. Snapshot of the quasiliquid surface phase at  $T=566$  K. Dark colored balls refer to atoms in the topmost layer.

culated value for the in-plane surface diffusion coefficient ( $\sim 2 \times 10^{-5} \text{ cm}^2 \text{ sec}^{-1}$ ) at this temperature which is very similar to the experimental bulk liquid value of  $2.2 \times 10^{-5} \text{ cm}^2 \text{ sec}^{-1}$ .<sup>30</sup> The surface continues to disorder with increasing temperature and at 590 K, less than 20% of the orientational order remains, suggesting that the surface has a liquidlike character (see Fig. 5). Moreover, preliminary studies of  $\omega_{1/2}$ , the width at one-half height of the dynamic structure factor for the surface layer above 590 K, show a  $K^2$  dependence even for large wave vector  $\mathbf{K}$ .<sup>31</sup> This means that surface atoms exhibit a continuous random diffusion typical of a liquid, rather than by jumps.

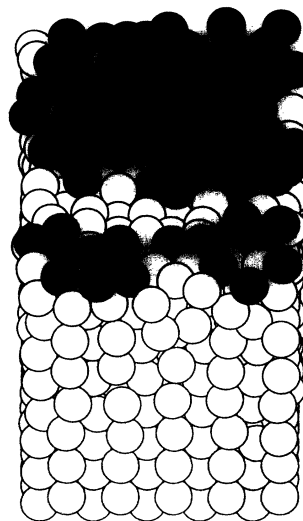


FIG. 5. Snapshot of the completely melted surface at  $T=590$  K. Dark colored balls refer to atoms in the topmost layer.

We examine next the long-ranged translational order by calculating the static structure factor for each layer, defined as

$$S(\mathbf{Q}) = \langle |\rho(\mathbf{Q})|^2 \rangle, \quad (5)$$

$$\rho(\mathbf{Q}) \equiv \frac{1}{N} \sum_{j=1}^N e^{-i\mathbf{Q} \cdot \mathbf{r}_j}, \quad (6)$$

where  $N$  is the number of atoms in the layer and  $\langle \dots \rangle$  stands for ensemble averages. For the rest of the paper,  $\mathbf{Q}$  is taken to be  $(2\sqrt{2}\pi/a, 2\pi/a, 0)$  where  $a$  is the lattice constant. From Fig. 6, we observe a gradual decrease in the intensity for the first layer below room temperature. This can be attributed to lattice vibrations as characterized by the Debye-Waller factor. Above 300 K, a sharp change in the gradient seems to indicate the onset of disordering first by vacancy-adatom pair creation as concluded above, followed by a saturation of the disorder in the surface layer above 500 K. This is consistent with the above results in that a liquidlike layer starts to form on the surface at this temperature. Incidentally, Speller *et al.*<sup>32</sup> have also observed, using low-energy ion scattering, that the disorder of the topmost layer is saturated at 480 K. For our case, deeper layers show a similar trend with the second layer achieving complete translational disorder (i.e.,  $S(\mathbf{Q}) \sim 0$ ) at 590 K. We thus conclude that we are actually witnessing a layer-by-layer disordering process. The important question at this stage is how important is the influence of the underlying crystal on the surface layer in the region 500–590 K. In fact, from the  $O_4$  results, the first layer still possesses a substantial amount of orientational order even though its  $S(\mathbf{Q})$  is near zero within this temperature range. One possible reason for this is the random creation and destruction of small (110)-like domains, thus effectively destroying the long-ranged translational order while still maintaining the short-ranged orientational order within these domains. Indeed, from Fig. 4, it can be seen that regions

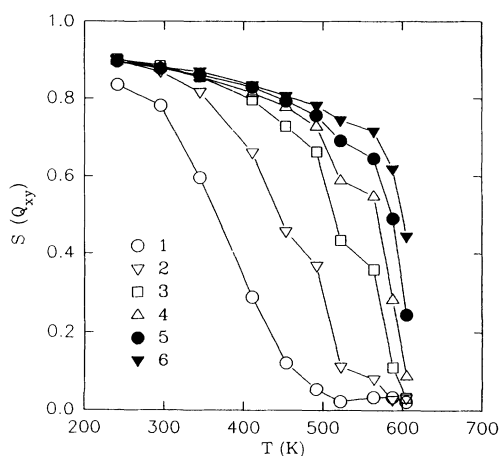


FIG. 6. Layer-resolved structure factor  $S(Q_{xy})$  versus temperature for the first six layers of our sample where  $Q_{xy} = (2\sqrt{2}\pi/a, 2\pi/a, 0)$ . Layer 1 refers to the topmost layer, layer 2 to the second, and so on.

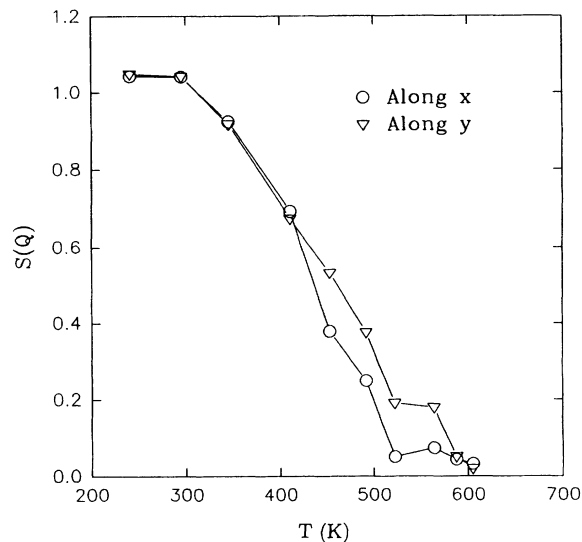


FIG. 7. Structure factor along  $x[\bar{1}\bar{1}0]$  and  $y[001]$  for the first layer as a function of temperature.

with (110)-like orientation are present. This can be understood in terms of a crystalline potential induced by the underlying layers. The residual order at the Pb(110) surface is found by Frenken and co-workers<sup>8</sup> to be manifested in the jump diffusion mechanism along  $[\bar{1}\bar{1}0]$  and  $[001]$ , the high value of the estimated activation energy and the pronounced anisotropy in the surface diffusion constant. Hence, surface atoms will have the tendency to arrange themselves into (110)-like facets even though they have a high diffusivity, thus preserving the short-ranged orientational order of the surface. As the temperature increases further, the second layer will start to disorder, resulting in a weakening of the crystalline field at the surface. To justify our explanation, we indeed observe that the translational order of the second layer vanishes at 590 K where the surface layer is believed to be liquid. Henceforth, we shall refer to a layer exhibiting

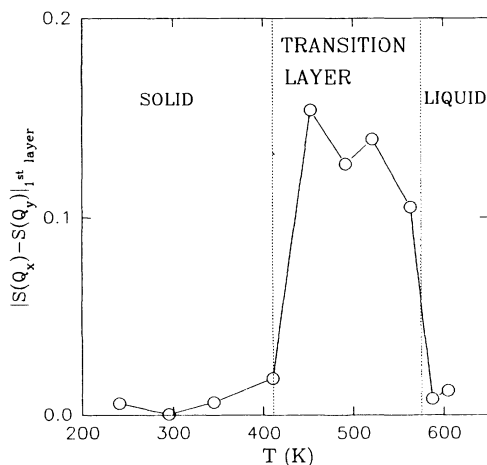


FIG. 8.  $|S(Q_x) - S(Q_y)|$  versus temperature for the topmost layer.

both crystalline and liquidlike properties as a QLL.

Recently, LEED and medium-energy ion-scattering (MEIS) experiments showed an anisotropy of the surface disordering process<sup>33,34</sup> which was not confirmed by other LEED experiments. To resolve this issue, we calculated the structure factor of the first layer for two reciprocal lattice vectors,  $Q_x = (2\pi/b)(1,0)$  and  $Q_y = (2\pi/a)(0,1)$ , where  $b = a/\sqrt{2}$  and  $a$  is the bulk lattice parameter.  $Q_x$  characterizes order of the layer in the closed-packed  $[1\bar{1}0]$  direction while  $Q_y$  characterizes order of the layer in the  $[001]$  direction, transverse to the closed-packed rows of atoms. We have fitted the low-temperature part of the curves to a Debye-Waller form  $\exp(-2W(g)T)$  and divide this part out of the original  $S(Q)$  curves as suggested by Prince, Breuer, and Bonzel.<sup>33</sup> From Fig. 7, it is clearly seen that  $S(Q_x)$  decreases faster than  $S(Q_y)$ . Furthermore, the temperatures at which both quantities become zero differ from each other by almost 100 K. This suggests that the disordering process is anisotropic and proceeds faster along the closed-packed  $[1\bar{1}0]$  direction. Recently, Frenken and co-workers<sup>8</sup> found that at

521 K, the order along the  $[001]$  direction is still complete, while the  $[1\bar{1}0]$  direction already exhibits a large degree of disorder. This seems to explain their observation that the diffusion along  $[1\bar{1}0]$  does not take place in jumps of single or multiple interatomic distances while along the  $[001]$  direction, jumps over single lattice spacing is the main diffusion mechanism. Molecular-dynamics simulation of diffusion on the premelted Pb(110) surface using the "glue" Hamiltonian (for the details see Ref. 31) is consistent with the above experimental results.

To get a different perspective of the surface disordering process, we plotted  $|S(Q_x) - S(Q_y)|$  versus  $T$  for the first layer as shown in Fig. 8. Above 400 K, the surface becomes rough due to the formation of adatoms, adclusters, and vacancies as shown earlier. This is accompanied by a sudden increase in  $|S(Q_x) - S(Q_y)|$ , indicating that the disordering process is anisotropic. This anomalous decrease in order along  $[1\bar{1}0]$  has been attributed to the formation of adatom-vacancy pairs as expected for the onset of surface roughening, as discussed in Ref. 6. However,

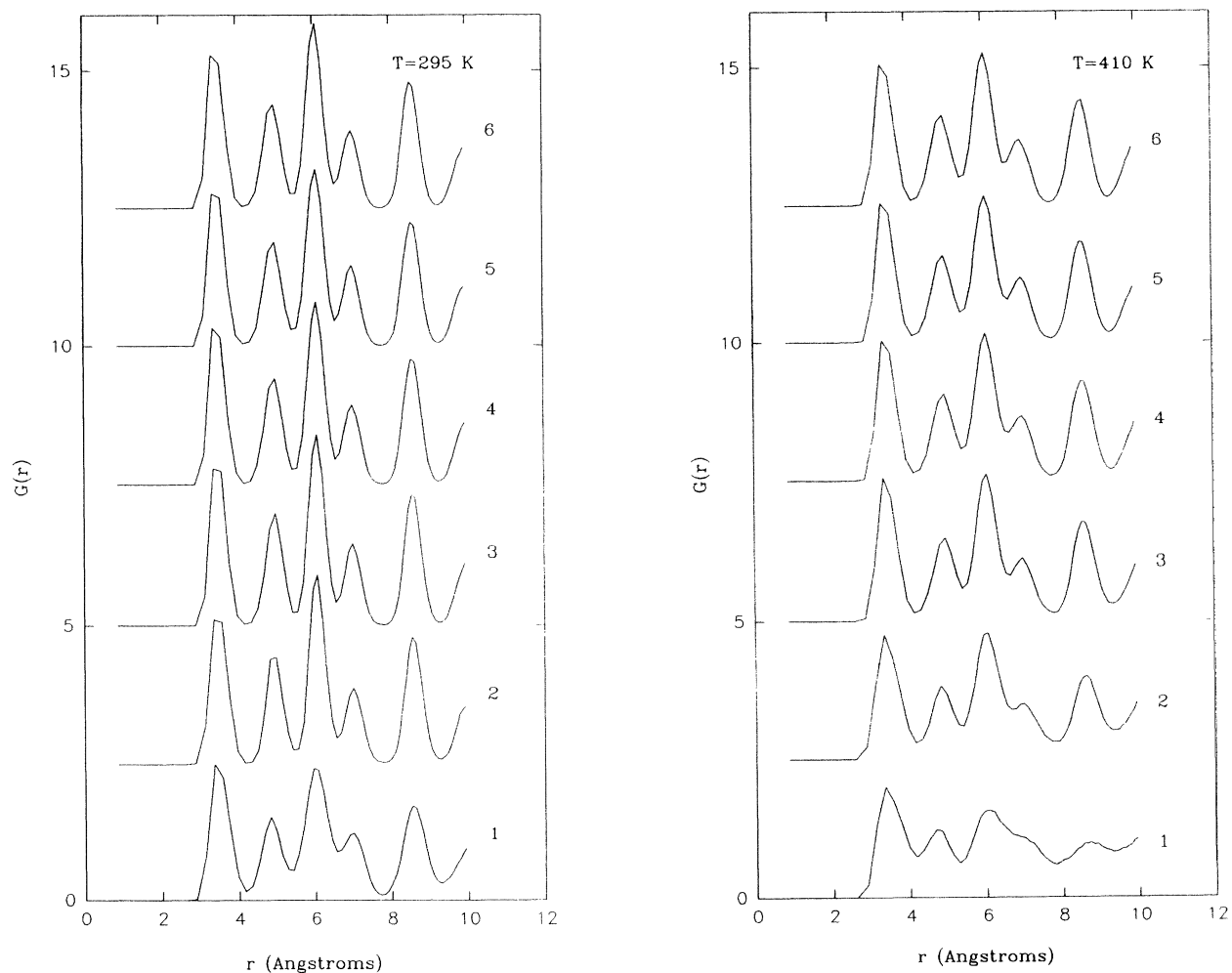


FIG. 9. The two-dimensional pair correlation function  $G(r)$  for the first six layers of our sample at  $T=295$ (a),  $410$ (b),  $453$ (c),  $491$ (d),  $521$ (e),  $566$ (f),  $587$ (g), and  $605$  K(h).

our small sample size and relatively short runs do not allow the determination of the roughening transition temperature  $T_r$ , although we can safely set a lower bound at 400 K, in good agreement with HRLEED studies. Recently, the roughening transition has been identified for Cu(110) by Häkkinen *et al.*<sup>35</sup> from a logarithmic divergence of the height-height correlation function, calculated using lattice-gas Monte Carlo methods with many-atom interactions derived from the effective-medium theory. Using molecular dynamics with identical interactions, they also showed that the roughening mechanism is connected with the formation of thermally generated diffusive clusters of both adatoms and vacancy type.

Between 430 and 590 K, an anisotropic phase (i.e., the transition layer) whereby structural order along the two orthogonal directions differs, is identified by a finite value of  $|S(Q_x) - S(Q_y)|$  (see Fig. 8). Below 500 K, this transition layer is "rough" but still crystalline since its  $S(Q)$  and  $O_4$  are finite while above that, liquidlike behavior is exhibited by a vanishing  $S(Q)$  and a diffusion coefficient comparable to the bulk liquid value as shown earlier (i.e., the quasiliquid phase). Finally at temperatures higher

than 590 K, the surface layer becomes a "true" isotropic liquid.

In addition to structure factors, we have calculated two-dimensional pair correlation functions  $G(r)$  for the first six layers for different temperatures as shown in Figs. 9(a)–9(h). It is clear that the crystallographic order of the surface disappears gradually as  $T_m$  is approached. Above 491 K, only short-range order is present on the surface, in agreement with the  $S(Q)$  data. At 605 K, the number of disordered layers has increased to three or four although the exact nature of such layers, whether quasiliquid or liquid, cannot be distinguished from  $G(r)$  data alone since both phases possess some degree of short-ranged order. We can, however, safely conclude that premelting (or the gradual loss of crystalline order) on Pb(110) occurs at  $\sim 500$  K, in good agreement with the above results. To summarize, our results indicate a possible roughening transition at or above 400 K, followed by premelting at  $\sim 500$  K ("rough"  $\rightarrow$  quasiliquid). The first layer is melted at 590 K (quasiliquid  $\rightarrow$  liquid) as evidenced by the complete loss of structural anisotropy as well as near zero values for both  $O_4$  and  $S(Q)$ .

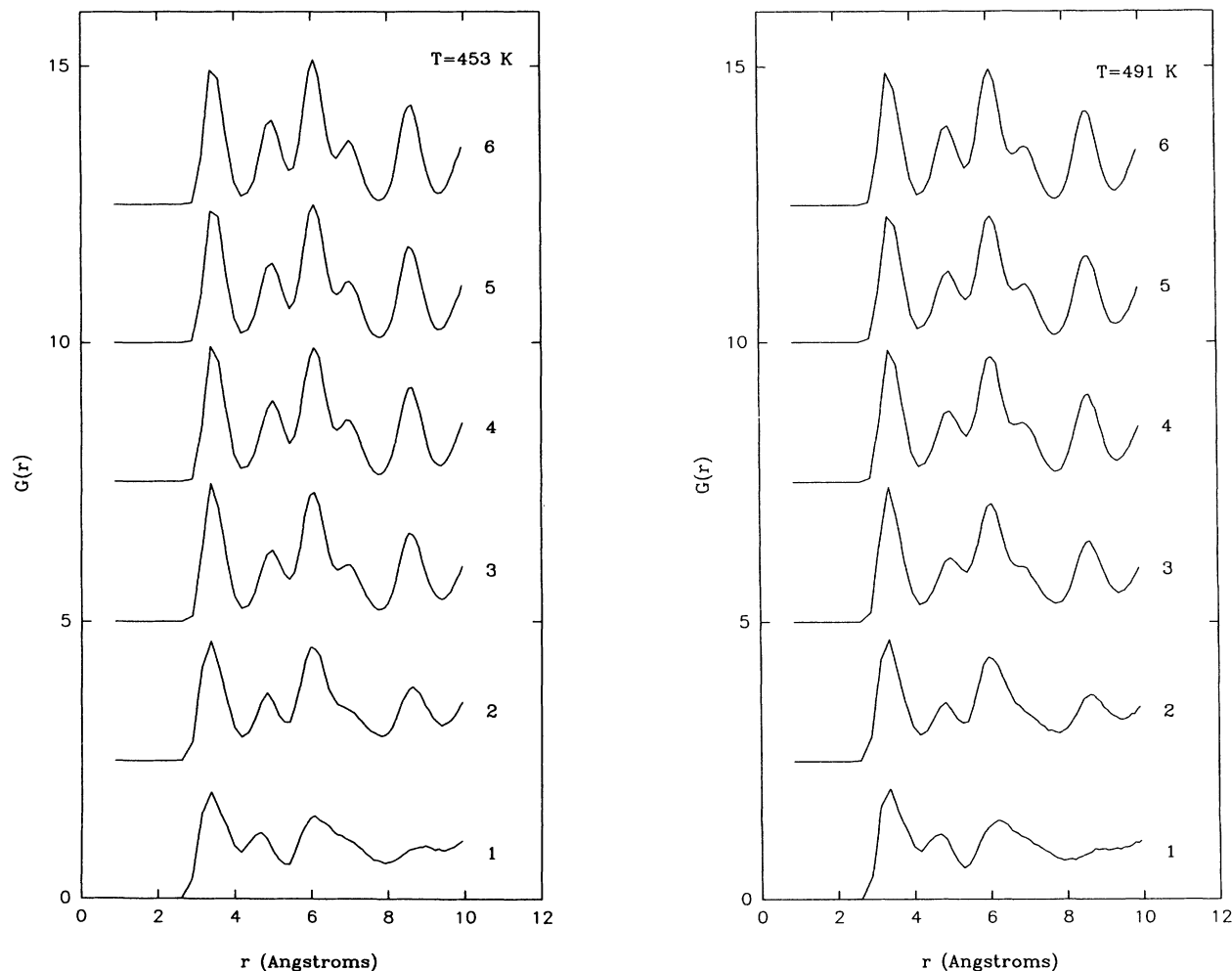


FIG. 9. (Continued).

### C. Surface stress

The surface stress of the fully relaxed (110) slab  $g$  is computed as the average value of the  $xx$  and  $yy$  components of the surface stress tensor  $g_{\alpha\beta}$ , defined as the strain derivative of the total free energy required to form the surface,

$$g_{\alpha\beta} = \frac{1}{A} \frac{\partial(A\gamma)}{\partial\epsilon_{\alpha\beta}} = \gamma\delta_{\alpha\beta} + \frac{\partial\gamma}{\partial\epsilon_{\alpha\beta}}, \quad (7)$$

where  $A$  is the surface area,  $\gamma$  the surface free energy,  $\epsilon_{\alpha\beta}$  an in-plane strain,  $\delta_{\alpha\beta}$  the Kronecker symbol, and  $\alpha, \beta = x, y, z$ . For the glue model used here, we obtained a value of  $92.8 \text{ meV}/\text{\AA}^2$  for the average stress at 0 K which is both positive (tensile) and large. The stress perpendicular to the surface is eliminated by relaxation but the lateral stress is still high though it is considerably less than the corresponding unrelaxed surface. The reason that the initial value of the stress is tensile is that the lower coordination of the surface atoms results in a larger contribution to the many-body term from surface atoms as com-

pared to bulk atoms. As a consequence, the surface wishes to contract to improve coordination and achieve a more stable configuration. One way is to undergo an inward relaxation, thus shortening the bonds between the top and second layer. This will continue until the vertical component of the stress tensor vanishes. However, the in-plane stress in the surface is mainly due to bonds within the top layer which do not shorten during relaxation because the surface of a semi-infinite solid is kept fixed at the bulk lattice parameter by the underlying crystal. As long as the surface density or coordination is less than the bulk, the tensile stress will never be eliminated. Measurements<sup>36</sup> and recent calculations<sup>20,27,37-39</sup> show that large tensile stresses are to be expected on many metal surfaces. For the (110) surface, the components of stress perpendicular and along the close-packed rows are different because of the anisotropic structure. It is smaller along the close-packed rows, in good agreement with *ab initio* calculation.<sup>37</sup>

Next, we look at the average stress as well as the stress anisotropy, defined as  $\Delta g = |g_{xx} - g_{yy}|$  as a function of temperature. From Fig. 10, it is clear that the stress an-

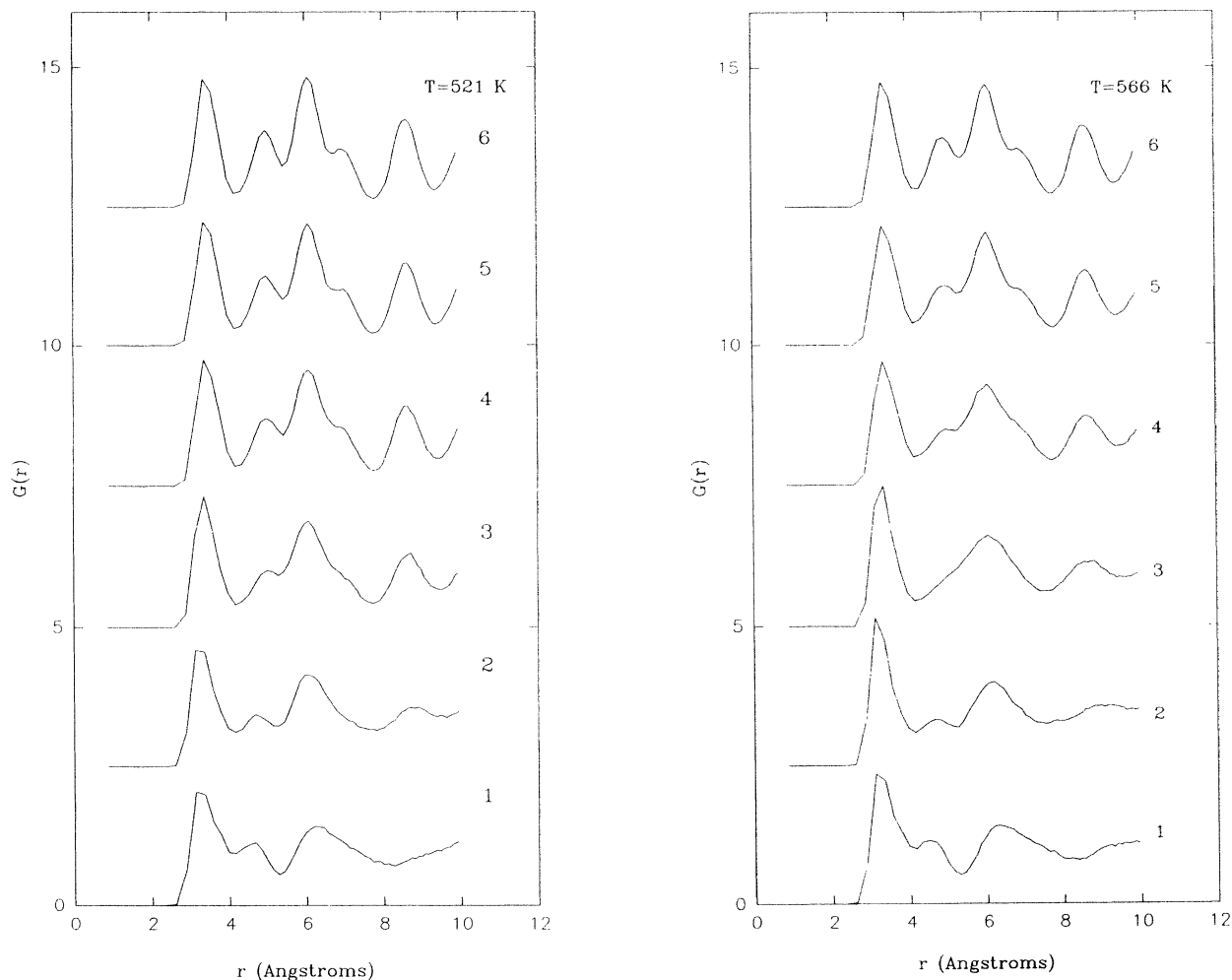


FIG. 9. (Continued).



isotropy vanishes above 590 K, indicating the presence of an isotropic layer on the surface which is earlier defined to be the liquid. The surface stress also shows anomalies at about 500 and 590 K (see Fig. 11) and since it is related to the surface free energy, we suspect that they are signals of first-order transitions. This seems to relate well to the rough  $\rightarrow$  quasiliquid and quasiliquid  $\rightarrow$  liquid transition as discussed previously. Pavlovska and Bauer<sup>41</sup> also reported the transition of the surface layer to a true liquid at 590–593 K by observing sharp changes in the surface properties in their multimethod study. An anomaly in  $\Delta g$  between 400 and 450 K is due to the anisotropic disordering of the surface. For both  $g_{xx}$  and  $g_{yy}$ , their behavior can be explained as follows: Besides the anomalies corresponding to possible first-order phase transitions, we note a sudden increase and decrease of  $g_{xx}$  and  $g_{yy}$ , respectively, between 300 and 400 K which can be attributed to the formation of vacancy-adatom pairs. This is because any breaks along the closed-packed rows will cause the two atoms neighboring the vacancy to be subjected to an increased tensile stress along  $x$ . However, the adatom produced is located in between closed-packed

rows, thus providing a “bridge” between two atoms in adjacent rows which reduces the local tensile stress along  $y$ . Between 400 and 450 K, saturation of  $g_{xx}$  is observed which can be explained by the saturation of vacancy-adatom pair production. According to Rosato, Ciccotti, and Pontikis,<sup>40</sup> the saturation of defect concentration in the first layer implies that the structure of the surface changes when temperature increases and can be taken as a first qualitative indication of a surface roughening.

#### IV. CONCLUSIONS

In this work, we have presented a detailed study of the surface relaxation, disordering and stress on the Pb(110) surface using the molecular-dynamics method with a realistic many-atom potential. The main results can be summarized as follows: An enhancement of the thermal expansion coefficient is observed at the surface, in good agreement with recent experiments. The surface disorders first by anharmonic effects (up to 350 K), then by vacancy-adatom formation, and finally premelting near 500 K. Complete melting is achieved in the first layer at  $\sim 590$  K. Surface stress studies give indication that the

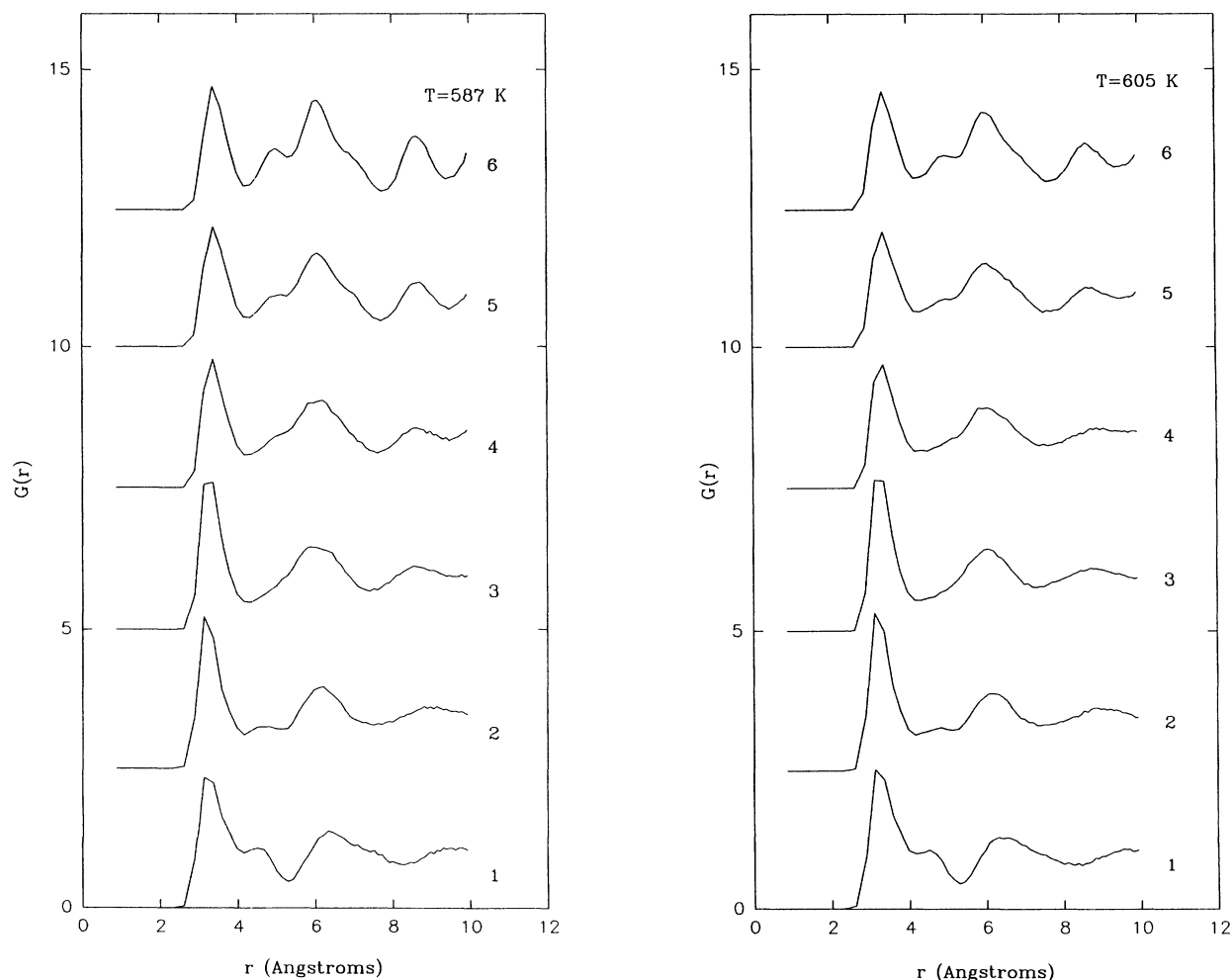


FIG. 9. (Continued).

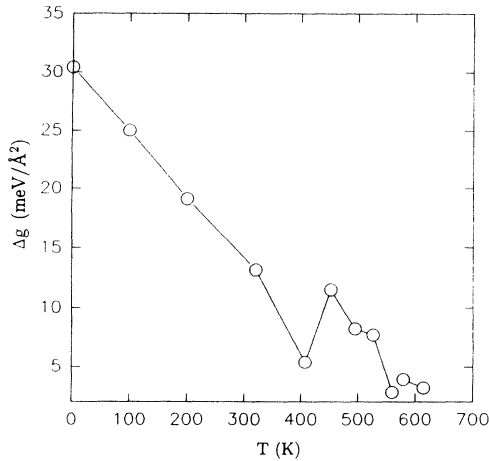


FIG. 10. Surface stress anisotropy  $\Delta g$  as a function of temperature.

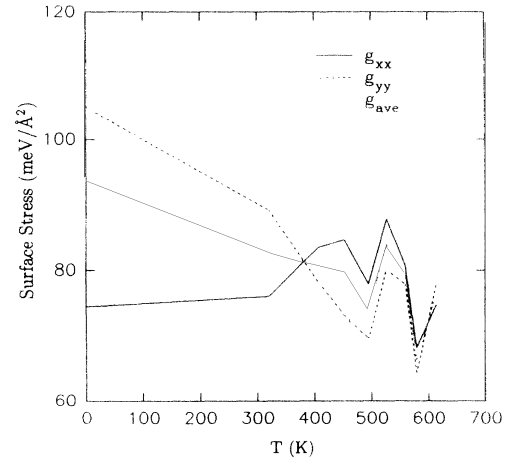


FIG. 11. Average surface stress and its components along  $x$  and  $y$  as a function of temperature.

transition from rough to quasiliquid as well as from quasiliquid to liquid phase is probably first order in nature. Further experimental work along this direction is clearly needed.

#### ACKNOWLEDGMENTS

The authors wish to thank E. Tosatti, E. Bauer, and J. W. M. Frenken for helpful discussions.

<sup>1</sup>J. C. Heyraud and J. J. Métois, *Surf. Sci.* **128**, 334 (1983).

<sup>2</sup>U. Breuer, K. C. Prince, H. P. Bonzel, W. Oed, K. Heinz, G. Schmidt, and K. Müller, *Surf. Sci. Lett.* **239**, L493 (1990).

<sup>3</sup>Y. S. Li, J. Quinn, F. Jona, and P. M. Marcus, *Phys. Rev. B* **40**, 8239 (1989).

<sup>4</sup>J. W. M. Frenken, F. Huussen, and J. F. van der Veen, *Phys. Rev. Lett.* **58**, 401 (1987).

<sup>5</sup>J. W. M. Frenken and J. F. van der Veen, *Phys. Rev. Lett.* **54**, 134 (1985); J. W. M. Frenken, P. M. J. Maree, and J. F. van der Veen, *Phys. Rev. B* **34**, 7506 (1986).

<sup>6</sup>U. Breuer, O. Knauff, and H. P. Bonzel, *Phys. Rev. B* **41**, 10848 (1990).

<sup>7</sup>B. Pluis, T. N. Taylor, D. Frenkel, and J. F. van der Veen, *Phys. Rev. B* **40**, 1353 (1989).

<sup>8</sup>J. W. M. Frenken, J. P. Toennies, and Ch. Wöll, *Phys. Rev. Lett.* **60**, 1727 (1988); J. W. M. Frenken, B. J. Hinch, J. P. Toennies, and Ch. Wöll, *Phys. Rev. B* **41**, 938 (1990); J. W. M. Frenken, B. J. Hinch, and J. P. Toennies, *Surf. Sci.* **211/212**, 21 (1989).

<sup>9</sup>L. Kuipers and J. W. M. Frenken, *Phys. Rev. Lett.* **70**, 3907 (1993).

<sup>10</sup>See, e.g., H. van Beijeren and I. Nolden, in *Structure and Dynamics of Surfaces II*, edited by W. Schommers and P. von Blanckenhagen (Springer, Berlin, 1987), p. 259.

<sup>11</sup>J. C. Heyraud and J. J. Métois, *J. Cryst. Growth* **82**, 269 (1987).

<sup>12</sup>H.-N. Yang, T.-M. Lu, and G.-C. Wang, *Phys. Rev. Lett.* **63**, 1621 (1989).

<sup>13</sup>J. M. Kosterlitz and D. J. Thouless, *J. Phys. C* **6**, 1181 (1973).

<sup>14</sup>K. Fang, H.-N. Yang, and G.-C. Wang, *Surf. Sci. Lett.* **284**, L399 (1993).

<sup>15</sup>A. Pavlovskaya and E. Bauer, *Europhys. Lett.* **9**, 797 (1989); A. Pavlovskaya, H. Steffen, and E. Bauer, *Surf. Sci.* **234**, 143 (1990).

<sup>16</sup>H.-N. Yang, K. Fang, G.-C. Wang, and T.-M. Lu, *Europhys. Lett.* **19**, 215 (1992).

<sup>17</sup>K. Rommelse and M. den Nijs, *Phys. Rev. Lett.* **59**, 2578 (1987); M. den Nijs and K. Rommelse, *Phys. Rev. B* **40**, 4709 (1989); M. den Nijs, *Phys. Rev. Lett.* **64**, 435 (1990).

<sup>18</sup>P. Tibbitts, M. Karimi, D. Ila, I. Dalins, and G. Vidali, *J. Vac. Sci. Technol. A* **9**, 1937 (1991).

<sup>19</sup>M. Karimi, G. Vidali, and I. Dalins, *Phys. Rev. B* **48**, 8986 (1993).

<sup>20</sup>H. S. Lim, C. K. Ong, and F. Ercolessi, *Surf. Sci.* **269/270**, 1109 (1992); *Z. Phys. D* **26**, 545 (1993).

<sup>21</sup>G. Bilalbegović, F. Ercolessi, and E. Tosatti, *Europhys. Lett.* **17**, 333 (1992); **18**, 163 (1992).

<sup>22</sup>O. Tomagnini, F. Ercolessi, and E. Tosatti, *Surf. Sci.* **287/288**, 1041 (1993).

<sup>23</sup>E. Tosatti and F. Ercolessi, *Mod. Phys. Lett. B* **5**, 413 (1991), and references therein; F. Ercolessi, S. Iarlori, O. Tomagnini, E. Tosatti, and X. J. Chen, *Surf. Sci.* **251/252**, 645 (1991); P. Carnevali, F. Ercolessi, and E. Tosatti, *Phys. Rev. B* **36**, 6701 (1987).

<sup>24</sup>F. Ercolessi, M. Parrinello, and E. Tosatti, *Philos. Mag. A* **58**, 213 (1988).

<sup>25</sup>C. P. Toh, H. S. Lim, C. K. Ong, and F. Ercolessi (unpublished).

<sup>26</sup>A. R. Miedema, *Z. Metallk.* **69**, 287 (1978).

<sup>27</sup>D. Wolf, *Surf. Sci.* **226**, 389 (1990).

<sup>28</sup>C. S. Jayanthi, E. Tosatti, and L. Pietronero, *Phys. Rev. B* **31**, 3456 (1985).

<sup>29</sup>A. Hoss, M. Nold, P. von Blanckenhagen, and O. Meyer, *Phys. Rev. B* **45**, 8714 (1992).

<sup>30</sup>J. W. Miller, *Phys. Rev.* **181**, 1095 (1969).

<sup>31</sup>C. P. Toh, C. K. Ong, and F. Ercolessi (unpublished).

<sup>32</sup>S. Speller, M. Schlegelberger, A. Niehof, and W. Heiland, *Phys. Rev. Lett.* **68**, 3452 (1992).

- <sup>33</sup>K. C. Prince, U. Breuer, and H. P. Bonzel, *Phys. Rev. Lett.* **60**, 1146 (1988).
- <sup>34</sup>A. W. D. van der Gon, H. M. Van Pinxteren, J. W. M. Frenken, and J. F. van der Veen, *Surf. Sci.* **244**, 259 (1991).
- <sup>35</sup>H. Häkkinen, J. Merikoski, M. Manninen, J. Timonen, and K. Kaski, *Phys. Rev. Lett.* **70**, 2451 (1993).
- <sup>36</sup>C. Solliard and M. Flüeli, *Surf. Sci.* **156**, 487 (1985) (Au and Pt).
- <sup>37</sup>M. Mansfield and R. J. Needs, *Phys. Rev. B* **43**, 8829 (1991).
- <sup>38</sup>M. C. Payne, N. Roberts, R. J. Needs, M. Needels, and J. D. Joannopoulos, *Surf. Sci.* **211/212**, 1 (1989).
- <sup>39</sup>V. Bortolani, F. Ercolessi, E. Tosatti, A. Franchini, and G. Santoro, *Europhys. Lett.* **12**, 149 (1990).
- <sup>40</sup>V. Rosato, G. Ciccotti, and V. Pontikis, *Phys. Rev. B* **33**, 1860 (1986).
- <sup>41</sup>A. Pavlovska and E. Bauer, *Appl. Phys. A* **51**, 172 (1990).